Mono- and Polyunsaturated Fatty Acids Counter Palmitate-Induced Mitochondrial Dysfunction in Rat Skeletal Muscle Cells

Nisr, Raid; Shah, Dinesh; Hundal, Hari

Published in:
Cellular Physiology and Biochemistry

DOI:
10.33594/000000282

Publication date:
2020

Cellular Physiology and Biochemistry

Cell Physiol Biochem 2020;54:975-993
DOI: 10.33594/000000282
Published online: 1 October 2020
Accepted: 10 September 2020

Original Paper

Mono- and Polyunsaturated Fatty Acids Counter Palmitate-Induced Mitochondrial Dysfunction in Rat Skeletal Muscle Cells

Raid B. Nisr Dinesh S. Shah Harinder S. Hundal

Division of Cell Signalling and Immunology, Sir James Black Centre, School of Life Sciences, University of Dundee, Dundee, UK

Key Words
Mitochondria • Skeletal Muscle • Palmitoleate • Oleate • ROS

Abstract
Background/Aims: Sustained increases in the circulating concentration of saturated fatty acids (SFAs, e.g. palmitate (PA), as seen during obesity, induces a chronic low grade inflammatory state that has been linked to metabolic dysfunction in tissues such as skeletal muscle that is characterized by disturbances in mitochondrial function and heightened production of reactive oxygen species (ROS). In contrast, monounsaturated (MUFAs, e.g. palmitoleate, PO; oleate, OL) and certain polyunsaturated (PUFAs, e.g. linoleate, LO) fatty acids have been shown to protect against some of the harmful metabolic effects induced by SFAs although it currently remains unknown whether this protection is associated with improved morphological and functional changes in mitochondrial biology and redox status in skeletal muscle cells. The aim of the present study was to investigate this issue. ***Methods:*** Rat skeletal (L6) myotubes were subject to sustained 16h incubation with SFAs either alone or in combination with a MUFA (PO, OL) or PUFA (LO) prior to performing subcellular fractionation, immunoblotting, fixed/live cell imaging (for assessment of mitochondrial morphology and ROS) or analysis of real time mitochondrial respiration. ***Results:*** Incubation of L6 myotubes with PA or stearate (SFA, C18:0) but not laurate (a medium chain SFA, C12:0) induced a robust increase in proinflammatory NFkB signaling as judged by loss of IkBα and increased expression of IL-6. This heightened SFA-induced proinflammatory tone was associated with increased production of ROS (superoxide and hydrogen peroxide) and significant loss in proteins involved in mitochondrial biogenesis, respiration and morphology (i.e. PGC1α, SDHA, ANT1 and MFN2). Consistent with these changes, PA induced profound fragmentation of the mitochondrial network and a marked reduction in mitochondrial respiratory capacity. These changes were not evident in myotubes incubated with PO, OL or LO alone, and, strikingly, these MUFAs and PUFA not only negated the proinflammatory action of PA, but antagonised the biochemical, morphological and functional changes in mitochondrial biology and ROS production induced in myotubes

Professor Hari Hundal Division of Cell Signalling and Immunology, Sir James Black Centre, School of Life Sciences, University of Dundee, Dundee, DD1 5EH (UK)
Tel. +44 1382 384969, E-Mail h.s.hundal@dundee.ac.uk

by the sustained oversupply of PA. ***Conclusion:*** Our findings indicate that PO, OL and LO exhibit anti-inflammatory and antioxidant characteristics and, significantly, they can ameliorate SFA-induced disturbances in mitochondrial form and function. These observations may have important nutritional implications in developing strategies that could potentially help limit obesity-induced metabolic dysfunction in tissues such as skeletal muscle.

Introduction

Increased proinflammatory signalling has been linked with obesity-induced metabolic dysfunction and insulin resistance in tissues such as skeletal muscle, and is characterised by elevated production of cytokines such as interleukin-6 (IL-6) and tumour necrosis factor (TNFα) [1, 2]. An important driver of metabolic dysfunction under these circumstances is considered to be fatty acids, in particular saturated fatty acids (SFA, e.g. palmitate (PA)), whose circulating concentration is characteristically elevated during obesity [3] and which, unlike unsaturated fatty acids, have long been known to be less efficiently oxidised [4-6] and therefore more obesogenic [7]. Consequently, sustained oversupply of SFAs may result in their incomplete oxidation and accumulation as short chain acyl-carnitines [8] and/or greater partitioning into lipotoxic fatty acid-derived molecules (e.g. such as ceramide and diacylglycerol). Such molecules have been implicated in the induction of a proinflammatory response [1, 9-11] as well as impaired signalling downstream of the insulin receptor [12-15]. The ability of muscle cells to efficiently oxidise fatty acids is crucially dependent upon mitochondrial capacity which has been shown in numerous studies to be markedly reduced during obesity and diabetes [16-18]. Whether this loss in mitochondrial capacity is a cause or consequence of insulin resistance remains a matter of considerable debate [19, 20], but there is growing acceptance that insulin resistance induced by the sustained over provision of SFAs is closely associated with significant disturbances in mitochondrial energy homeostasis [17]. We have recently shown, for example, that skeletal muscle cells subject to fuel overloading with palmitate exhibit a profound increase in mitochondrial fragmentation and mitophagy that is accompanied by increased generation of reactive oxygen species (ROS), as well as a decline in the expression/abundance of proteins that influence both mitochondrial biogenesis and respiration that collectively may help account for the reduced mitochondrial respiratory capacity [21]. Significantly, these SFA-induced disturbances in mitochondrial morphology and function can be countered by pharmacological or genetic repression of the proinflammatory IKKβ-NFkB signalling axis, which also coincides with enhanced cellular responsiveness to insulin [21]. Previous studies in cultured skeletal muscle cells have also noted that palmitate exhibits a greater propensity to induce mitochondrial DNA (mtDNA) damage and that strategies that help mitigate this not only improve mitochondrial redox status, but serve to partially restore insulin sensitivity of muscle cells [22]. Such observations imply that the chronic low-grade inflammatory state that is seen in muscle during obesity may partly be instituted by the rise in circulating SFAs and, as such, may contribute to changes in mitochondrial form and function that result in the development and progression of insulin resistance in skeletal muscle.

In contrast, mono- or poly-unsaturated fatty acids (MUFAs and PUFAs) do not possess the same lipotoxic or pathogenic potential as that ascribed to SFAs and, remarkably, some unsaturated fatty acids (e.g. palmitoleate) have been shown to not only promote beneficial cellular and systemic effects on metabolic homeostasis [23-25], but also mitigate some of the harmful effects associated with SFA oversupply [26-28]. In 3T3-L1 adipocytes, for example, sustained exposure of cells to palmitoleate promotes greater mitochondrial energy expenditure as demonstrated by increased fatty acid oxidation and ATP synthesis, which is likely to be facilitated by the associated increase in the abundance of OXPHOS complexes [29]. Similarly, unsaturated fatty acids (palmitoleate, oleate and linoleate) also stimulate mitochondrial activity in human skeletal muscle cells; an effect that has been linked to the induction of PGC1α key transcriptional coactivator that stimulates mitochondrial biogenesis

and energy metabolism [30]. Furthermore, analysis of real time mitochondrial bioenergetics indicate that whilst SFAs reduce the coupling efficiency of oxidative phosphorylation in human myoblasts, unsaturated fatty acids (e.g. oleate) do not, thereby further supporting the idea that MUFAs are better tolerated and do not overtly impact on mitochondrial respiratory function [31]. In line with this, studies in cultured rat L6 muscle cells have shown that although oleate *per se* has no discernible effect on ROS production or mtDNA its provision antagonises the excessive generation of ROS, mtDNA damage and loss of insulin sensitivity induced by PA and that it may do so by promoting PGC1α expression/abundance, ATP levels and cell viability [32]. It is also noteworthy that recent work has shown that the ability of oleate to suppress production of proinflammatory cytokines *via* the canonical NFkB signalling pathway and mitochondrial superoxide production blunts PA-driven myocellular atrophy [33]. This latter observation implies that SFA-induced mitochondrial dysfunction may be a contributing factor in muscle atrophy and that MUFAs may have therapeutic value in restraining loss of muscle mass during conditions such as obesity and ageing by helping to preserve myocellular mitochondrial health [33]. In addition to stimulating mitochondrial activity, unsaturated fatty acids can also promote synthesis of neutral triglyceride (TAG) in myotubes [34, 35] and may also function as mild mitochondrial uncouplers [36]. These metabolic responses allow greater oxidation and/or partitioning of SFAs into an inert molecular species that may help off-set their availability for synthesis of lipotoxic fatty acid-derived intermediates. Precisely how MUFAs and PUFAs convey such benefits and how they might antagonise SFA-induced disturbances in metabolic function are not fully understood but we hypothesise that their anti-inflammatory action helps counter the deleterious impact that SFAs have upon mitochondrial form, respiratory function and ROS generation. The purpose of the studies reported herein was to test this hypothesis. In this study, we present novel data showing the differential impact that SFAs and unsaturated fatty acids have on mitochondrial morphology and bioenergetics and show that the capacity of MUFAs and PUFAs to ameliorate PA-induced mitochondrial dysfunction is associated with a suppression in proinflammatory signalling, ROS production but not a reduction in PA uptake.

Materials and Methods

Chemicals and reagents

Tisssue culture media (α-MEM, α-minimum essential medium) and serum (foetal bovine), Mitosox, prolong diamond antifade mountant, mitotracker dyes were all purchased from Thermo Fisher Scientific (UK). MitoSpy™ Green FM was from BioLegends (UK). MitoPYI, hepatocyte growth factor, laurate (C12:0), palmitate (C16:0), stearate (C18:0), palmitoleate (C16:1), oleate (C18:1), linoleate (C18:2), oligomycin, FCCP (carbonyl cyanide p-trifluoromethoxyphenylhydrazone), rotenone, antimycin-A, hygromycin B, human, SYBR® Green JumpStart Taq Ready Mix were all purchased from Sigma Aldrich, UK). [^{3}H]-palmitic acid was obtained from PerkinElmer Life Sciences.

L6 skeletal muscle cell culture and fatty acid treatment

L6 muscle cells were cultured in α-minimal essential media (αMEM) containing 2% (v/v) foetal bovine serum (FBS) and 1% (v/v) antibiotic/antimycotic solution (100 units/ml penicillin, 100 μg/ml streptomycin, 250 ng/ml amphotericin B) in a humidified atmosphere of 95% air and 5% CO_2 at 37°C and allowed to differentiate into myotubes as previously described in serum-containing media with glucose (5 mM) [37]. For fatty acid treatments a 100 mM stock solution of the appropriate fatty acid was prepared in absolute ethanol as previously reported [38, 39]. This stock was subsequently diluted to a final concentration as indicated in the figure legends by addition to culture media containing 2% (w/v) fatty acid free BSA and allowed to precomplex for 1h at 37°C before being applied onto myotubes. Based on previous work from our group assessing dose- and time-dependent responses of palmitate that induced maximally effective changes in proinflammatory NFkB signalling, ROS generation and insulin signalling [21, 34] (also see Supplementary Fig. S1 and S2 – for all supplementary material see www.cellphysiolbiochem.com), myotubes were incubated with 0.4 mM palmitate for 16h in the absence and presence of unsaturated fatty acids (palmitoleate

(PO, C16:1), Oleate (OL, C18:1) or linoleate (LO, C18:2)) at concentrations and for periods indicated in the figure legends. Given that muscle cells in the current studies were used as fully differentiated myotubes, it worth stating that treatment with palmitate and unsaturated fatty acids at the concentration and incubation period indicated did not adversely affect myotube viability as judged by analysis of total cell protein to DNA content (Supplementary Fig. S2C).

Quantitative real time PCR, mitochondrial DNA quantification and mitochondrial isolation

Following appropriate treatments with fatty acids and/or fluorescent dyes as indicated in the figure legends, L6 myotubes were prepared for RNA extraction and qPCR analysis as described previously [21]. In brief, the TRizol method (Thermo Fisher Scientific, UK) was used to isolate total RNA from myotubes from which cDNA was prepared using a qScript cDNA synthesis kit as per manufacturer's instructions and real time PCR Syber Green method subsequently used to quantify IL-6 and actin mRNA using the following qPCR primer sequences: IL-6, forward 5' AGCCACTGCCTTCCCTACTT 3' and reverse 5' GCCATTGCACAACTCTTTTCTC 3'; Actin, forward 5' TGGAGAAGATTTGGCACCACAC 3' and reverse 5' CAGAGGCATACAGGGACAACAC 3'. The abundance of mitochondrial DNA (mtDNA) was used as a proxy for mitochondrial mass. Total DNA was extracted from L6 myotubes using a Qiagen DNaesy kit and mtDNA quantified using qPCR primers directed against the mitochondrial ND4 gene (Forward 5' GAGGCAACCAAACAGAACGC 3' and Reverse 5' ATCATGTTGAGGGTAGGGGGT 3') and the nuclear-encoded COX4 gene (Forward 5' AATGTTGGCTACCAGGGCAC 3' and Reverse 5' GGGTAGTCACGCCGATCAAC 3') using the Syber Green method. Data was expressed as a ratio of the ΔΔCt ND4 to the ΔΔCt of COX4. For analysis of mitochondrial proteins, a mitochondria isolation kit (#89874, Thermo Fisher Scientific) was used to prepare a mitochondrial enriched membrane fraction from L6 myotubes as per manufacturer's instructions.

SDS-PAGE and immunoblotting

Cell lysates, cytosolic or mitochondrial enriched fractions (20 μg protein) from muscle cells were subjected to SDS/PAGE on 10% resolving gels and transferred onto polyvinylidene difluoride (PVDF) membranes (Millipore, Harts, UK), as described previously [37]. Membranes were immunoblotted with the following antibodies: actin (#A5060) and tubulin (#T6074) were obtained from Sigma; ANT-1 (#ab180715), IkBα (#SC-371), SDHA (#SC98253) and GAPDH (#SC32233) were purchased Santa Cruz; TOM20 (#42406S), COX4 (#4580S), Catalase (#14097) and SOD2 (#D9V9C) were all purchased from Cell Signalling Technology; UCP3 (#GTX112699) from Genetex; TFAM (ab131607), NRF1 (#ab175932), NRF2 (#ab92946) and PGC1α (#ab54481) were from Abcam. Primary antibody detection was performed using appropriate horseradish peroxidase (HRP) conjugated secondary mouse (#7076S) or rabbit (#7074S) antibodies were purchased from Cell Signalling Technology and visualized using enhanced chemiluminescence (Pierce-Perbio Biotech, Tattenhall, UK) on Kodak X-OMAT film (Eastman-Kodak, Rochester, UK) or digital images acquired using the LICOR system. Immunoreactive protein bands were quantified using ImageJ Software.

Analysis of Reactive Oxygen Species (ROS)

Fluorescence probes were used for detection and quantification of ROS. For analysis of superoxide, L6 myotubes were subject to experimental treatments as indicated in the figure legends prior to a 30 min incubation with 5 μM MitoSox in a humidified atmosphere of 95% air and 5% CO_2 at 37°C. Mitosox is specifically targeted to mitochondria in live cells and its oxidation by superoxide produces red fluorescence that was quantified using a CLARIOstar plate reader with absorption/emission maxima at 510/585 nm as per instructions from the manufacturer (ThermoFisher Scientific).

For analysis of hydrogen peroxide (H_2O_2), muscle cells were incubated with 5 μM MitoPYI (a mitochondrial targeted H_2O_2 probe) and 1 μM deep red cell tracker in a 37°C incubator with a humidified atmosphere of 95% air and 5% CO_2 for 45 min. Myotubes were subsequently imaged using a Zeiss confocal microscope with excitation/emission maxima for MitoPYI set to 488/530 nm and that for the cell tracker at 633/647 nm. Microscope images were analysed to quantify fluorescence generated by MitoPYI from at least 8-10 random visual fields (40-50 myotubes) per condition per experiment using ImageJ software.

Analysis of cellular respiration and mitochondrial energetics

A Seahorse XF24 analyser was used to analyse respiration by measurement of oxygen consumption rates (OCR) in L6 myotubes. Muscle cells were cultured on Seahorse culture plates in serum-containing

media supplemented with 5 mM D-glucose and/or fatty acids at concentrations indicated in the figure legends for 16 h prior to analyses of basal, ATP-Linked and maximal respiration and non-mitochondrial oxygen consumption achieved by the addition of oligomycin (1 μM), FCCP (carbonyl cyanide 4-(trifluoromethoxy) phenylhydrazone) (2 μM), rotenone (1 μM) and Antimycin (2 μM) at times indicated on the OCR traces. Mitochondrial respiration rates were normalised to cell protein within the culture wells of the Seahorse plate [21].

Palmitate uptake in L6 myotubes

Fatty acid uptake was assayed in L6 myotubes as described previously [23, 34]. Myotubes were cultured in twelve-well dishes and incubated with 0.4mM [^{3}H]-palmitic acid (1μCi/mL) in the absence and presence of 0.4mM oleate for periods up to 2 h as indicated in the figure and legend. At the specified time periods uptake was terminated by rapid aspiration of uptake buffer and myotubes washed twice with ice-cold 0.9% (w/v) NaCl prior to lysis with 50mM NaOH. Radioactivity in muscle cell lysates was subsequently quantified by liquid scintillation counting.

Analysis of mitochondrial morphology

Mitospy Green (BioLegend, UK) FM was used to investigate effects of fatty acid treatments upon mitochondrial morphology using fixed or live cell imaging as previously described [21]. Briefly, L6 myotubes were grown on glass coverslips (15 mm^2) prior to incubation with fatty acids for times and at concentrations indicated in the figure legends. At the end of such treatments, myotubes were washed and subsequently maintained in fresh media containing 300 nM Mitospy for 30 min at 37°C in a 95% O_2/5% CO_2 environment. After treatment with Mitospy, cells were washed and subsequently fixed with 2% (w/v) paraformaldehyde and mounted in prolonged diamond antifade before being visualised using a Zeiss confocal microscope. For some experiments, myotubes were grown on 8 well chamber slide plates (Ibidia, UK) and following appropriate treatment with fatty acids were washed with fresh phenol red free media prior to incubation with Mitospy. Live cell imaging of mitochondrial morphology was then performed using Zeiss confocal microscope at 37°C in a 5% CO_2 chamber with excitation/emission set at 480nm and 520nm. ZEISS ZEN microscope software or ImageJ was then used to quantify mitochondrial length. To reduce potential bias, at least 50 myotubes were analysed within 10 randomly chosen fields for each experimental condition tested. Mitochondrial morphology within myotubes was categorised as either tubular/elongated (including as part of a network) when mitochondrial length was greater than 1 μm or spheroid/fragmented if mitochondria were 1 μm or less in length. The proportion of mitochondria falling into each category was then expressed as a percentage.

Statistical analysis

Where appropriate, details of the number of experimental replicates within a single experiment and the number of times each experiment was performed are detailed in the individual figure legends. Statistical analysis was performed using GraphPad Prism version 7 software using one-way analysis of variance (ANOVA) and Tukey post hoc test for multiple comparisons. Values were considered significant at $P < 0.05$.

Results

Saturated fatty acids induce proinflammatory NFkB signalling and mitochondrial dysfunction in a chain length dependent manner

We have recently shown that myotubes subjected to a sustained period of exposure to 0.4 mM palmitate (PA), a C16:0 SFA, exhibit heightened NFkB proinflammatory signalling, which is mechanistically linked to increased mitochondrial fragmentation and impaired mitochondrial respiratory function [21]. What is not known is whether this SFA-induced mitochondrial dysfunction is chain length dependent and whether it is also a feature associated with myotube exposure to unsaturated fatty acids. Fig. 1A shows that myotubes exposed to 0.4 mM PA or stearate (ST, a C18:0 SFA) for 16 h in media also containing 5 mM D-glucose exhibit increased NFkB activation as judged by the loss of IkBα and elevated expression of IL-6, an NFkB gene target. Strikingly, this increased proinflammatory drive was not observed

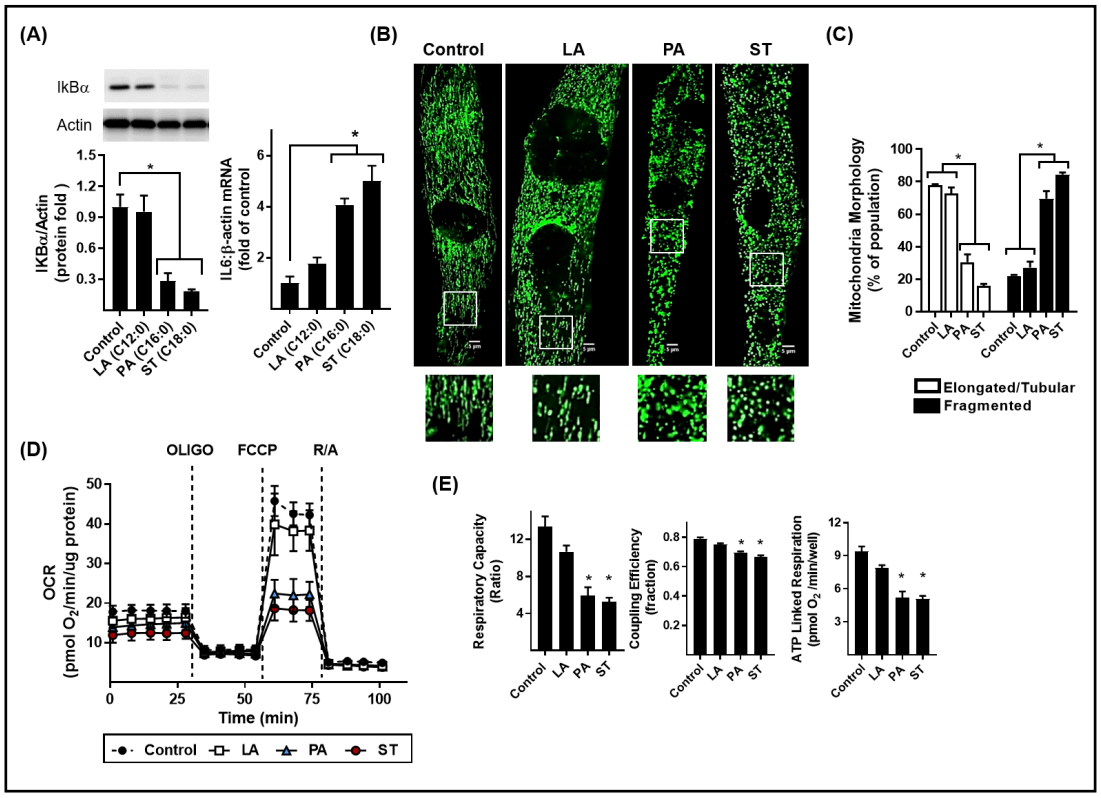

Fig. 1. Effects of fatty acyl chain saturation on NFkB signalling, mitochondrial morphology and cellular respiration in L6 myotubes. L6 myotubes were incubated in media containing D-glucose (5 mM) in the absence and presence of saturated fatty acids laurate (LA, C12:0), palmitate (PA, C16:0) or stearate (ST, C18:0) for 16 h prior to analysis of: (A) cellular IkBα abundance by immunoblotting and IL6 and β-actin mRNA abundance by qPCR; (B) analysis and quantification of mitochondrial morphology assessed by mitotracker green (mitospy) staining and confocal microscopy. The white boxed areas are magnified to show differences in morphology, the scale bar in the main visual fields represents 5 µm. (C) Mitochondrial morphology (elongated versus fragmented) was subsequently quantified using ImageJ software. For analysis of real-time cellular respiration in L6 myotubes we used a Seahorse XF24 analyser. L6 myotubes were incubated for 16 h with either GLC (5 mM) alone (control) or glucose co-supplemented with 0.4 mM of either LA, PA or ST. Oligomycin (1 µM), FCCP (1 µM) and a rotenone (1 µM)/antimycin-A (2 µM) mix were added at times indicated by the dotted lines on the Seahorse trace. The trace shown in (D) is a representative readout of oxygen consumption rate (OCR) from a single experiment with time point (mean ± SD) representing a triplicate measurement. The data shown in (E) indicates the respiratory capacity ratio, coupling efficiency of oxidative phosphorylation and ATP linked respiration respectively (5 determinations/condition/experiment). The graphical data shown in (A, C and E) are the combined analyses of three separate experiments and represent mean ± SEM. Asterisks indicate a significant change ($P<0.05$) to the control condition or between the indicated bars.

in myotubes incubated with an equivalent concentration of laurate (LA), a medium chain (C12:0) SFA (Fig. 1A). Furthermore, the activation of the NFkB pathway by PA and ST was associated with a profound change in mitochondrial morphology that was visualised by live cell imaging in which mitochondria were stained using Mitotracker Green. The dye accumulates within mitochondria but does not penetrate nuclei, which, consequently, become highlighted by virtue of dye exclusion. Fig. 1B and 1C show that myotubes not subjected to any prior fatty acid treatment exhibit mitochondria that are predominantly (~80%) organised as part of an elongated/tubular network (in which mitochondrial length was equal to or greater than 1 um as determined using ImageJ software), whereas they become highly fragmented and spheroid in nature (~70%) upon myotube treatment with PA and, more

so (~80%) when incubated with ST (Fig. 1C). In contrast, such fragmentation was not apparent in myotubes that had been incubated with LA. Consistent with the idea that a fragmented mitochondrial morphology may be associated with reduced bioenergetic efficiency, analysis of mitochondrial respiration revealed that both PA and ST significantly reduced the cellular oxygen consumption rate (OCR) and that this was associated with a decline in respiratory capacity, coupling efficiency and ATP-linked respiration within myotubes (Fig. 1D and 1E). In contrast, LA, which did not induce any notable changes in proinflammatory NFkB signalling or mitochondrial fragmentation, did not impact significantly on these bioenergetic parameters (Fig. 1D and 1E).

Effects of Mono- and poly-unsaturated fatty acids on PA-induced proinflammatory signalling, PA uptake, mitochondrial morphology and respiration

Unlike PA, sustained (16 h) incubation of L6 myotubes with MUFAs, palmitoleate (PO, C16:1) and oleate (OL, C18:1), or the PUFA, linoleate (LO, C18:2), did not induce an increase in NFkB signalling based on analysis of IkBα abundance and IL6 gene expression as readout (compare lanes 6-8 with lane 2, Fig. 2A and 2B). Significantly, however, all three fatty acids were found to repress the proinflammatory drive observed with over-supply of PA (compare lanes 3-5 with lane 2, Fig. 2A and 2B, and Supplementary Fig. S1). It is plausible that unsaturated fatty acids may restrain the proinflammatory action of PA by competitively inhibiting its uptake *via* a common cell surface fatty acid transporter. To test this possibility, we assayed uptake of radiolabelled PA in the absence and presence of a competing concentration of OL. Fig. 2C shows that we observed a time-dependent increase in PA uptake by myotubes that, strikingly, was further augmented in the presence of 0.4 mM OL thus negating the idea that OL restrains the proinflammatory effect of PA by suppressing its uptake.

Given that SFA-induced proinflammatory signalling is associated with disturbances in mitochondrial form and function [21], we subsequently performed live cell imaging of myotubes stained with Mitotracker Green to assess the effects of MUFA/PUFA provision on

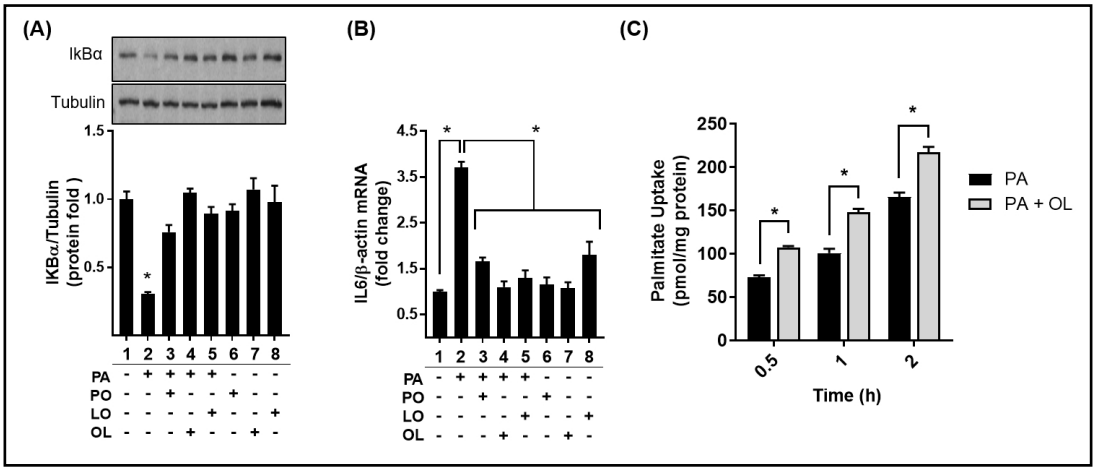

Fig. 2. Effect of unsaturated fatty acids on palmitate induced NFkB proinflammatory signalling and palmitate uptake. L6 myotubes were incubated for 16 h in media containing D-glucose (5 mM) supplemented with or without palmitate (PA, 0.4 mM) or unsaturated fatty acids palmitoleate (PO, C16:1), Oleate (OL, C18:1) or linoleate (LO, C18:2) at 0.4 mM as indicated prior to analysis of (A) cellular IkBα abundance by immunoblotting and (B) IL6 and β-actin mRNA abundance by qPCR. The data represent the combined analyses of four separate experiments. For PA uptake (C), myotubes were incubated in uptake buffer containing 0.4 mM PA and [3H]-PA (1 mCi/ml) palmitate in the absence and presence of 0.4 mM OL for times indicated. Data in panels A and B are from three separate immunoblotting/qPCR experiments, whereas the uptake data is from six separate experimental determinations. Data is presented as mean ± SEM. Asterisks indicate a significant change ($P<0.05$) to the control condition (lacking any fatty acid additions) or between the indicated bar values.

mitochondrial morphology. Consistent with recent work from our lab [21] and the data presented in Fig. 1B, PA induced a marked increase in mitochondrial fragmentation that was not apparent in myotubes incubated with PO, OL or LO alone in which mitochondria were predominantly (70-80%) tubular/elongated in form (Fig. 3A and 3B). Strikingly, the increase in mitochondrial fragmentation induced by PA was significantly blunted upon co-exposure of myotubes with either PO, OL or LO. We have previously reported that the PA-induced fragmentation of the mitochondrial network is notably associated with a cellular reduction in mitofusin-2 (MFN2) content, an outer mitochondrial membrane GTPase that critically helps support mitochondrial fusion [21]. Analysis of MFN2 abundance in a mitochondrial-enriched membrane fraction showed that relative to untreated myotubes those incubated

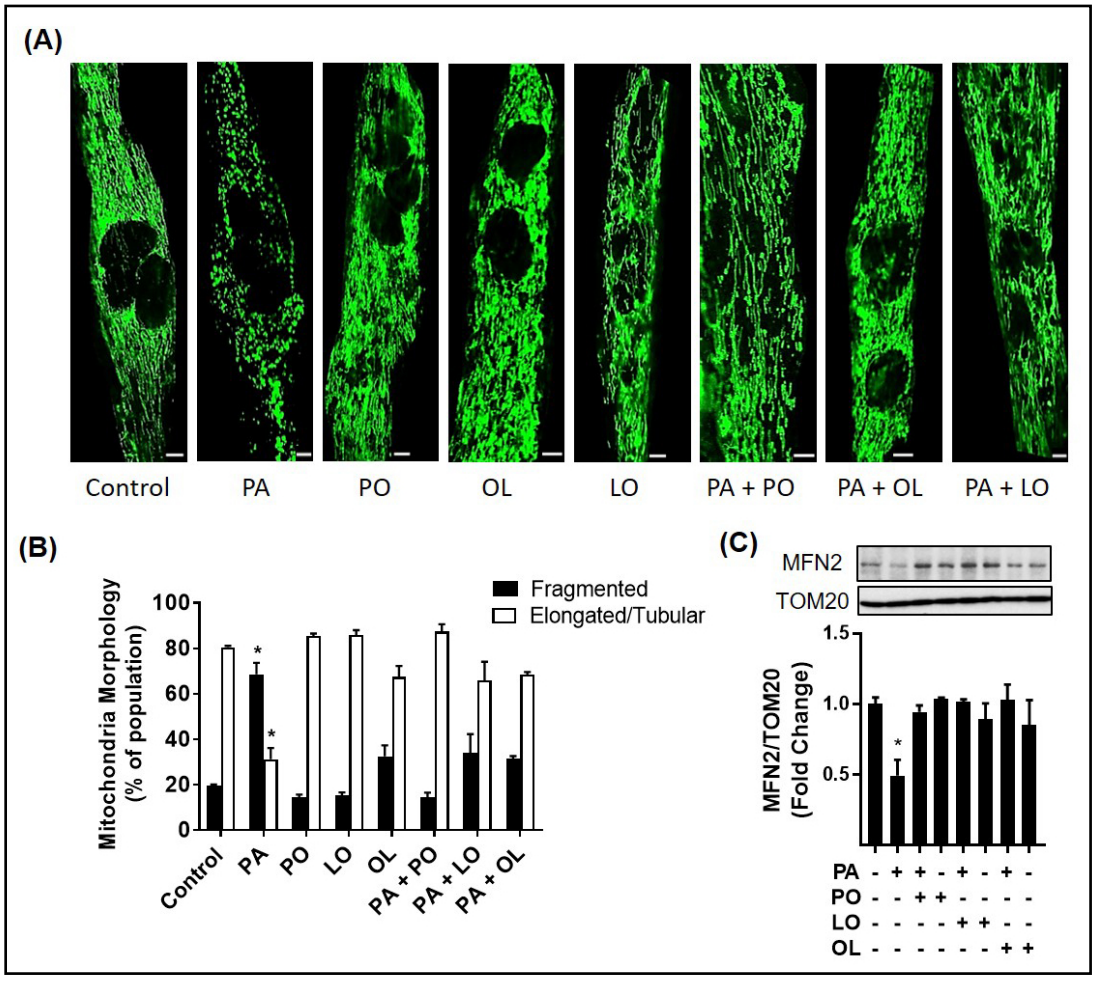

Fig. 3. Effect of palmitate and/or unsaturated fatty acids on mitochondrial morphology. L6 myotubes were incubated for 16 h in media containing D-glucose (5 mM) supplemented with or without palmitate (PA, 0.4 mM) or unsaturated fatty acids palmitoleate (PO, C16:1), Oleate (OL, C18:1) or linoleate (LO, C18:2) at 0.4 mM as indicated prior to: (A) mitotracker green (mitospy) staining and live cell imaging by confocal microscopy of L6 myotubes (the scale bar represents 5 μm); (B) analysis of mitochondrial morphology (elongated versus fragmented) was quantified using ImageJ software and presented as elongated/tubular if mitochondria were >1 μm or fragmented if <1 μm in length and (C) Immunoblotting and quantification of mitofusin 2 (MFN2), a key regulator of mitochondria dynamics in a mitochondrial-enriched fraction. The abundance of TOM20 a mitochondrial marker protein was used as a gel loading control. The bar graph represents quantitative analysis of MFN2 abundance relative to TOM20 with data presented as mean ± SEM from a minimum of 4 separate experiments. The asterisk indicates a significant change ($P<0.05$) to the control condition (lacking any fatty acid additions).

with PA exhibit ~50% loss in MFN2, but this was averted upon co-treatment of myotubes with MUFAs or PUFA (Fig. 3C).

Given that morphological changes in mitochondrial form caused by PA oversupply could be restrained by co-provision of PO, OL and LO we subsequently tested whether these fatty acids could also mitigate disturbances in mitochondrial respiration induced by PA in myotubes. Fig. 4A depicts a real time OCR trace from a single experiment in which each time point represents data from a triplicate measure. The trace shows that whilst sustained preincubation of myotubes with 0.4 mM PA treatment suppresses the OCR, incubating myotubes with equivalent concentrations of PO, OL or LO did not cause any significant deviation in OCR from that assayed in untreated myotubes. Significantly, all three unsaturated fatty acids antagonised the PA-induced reduction in basal and ATP-linked respiration and partially ameliorated the loss in maximal respiratory capacity (Fig. 4B). The reduced respiratory capacity seen in myotubes in response to PA oversupply could not be accounted for by a reduction in mitochondrial mass given that we observed no significant change in mitochondrial DNA in response to treatment with any of the fatty acids we used (Fig. 4C).

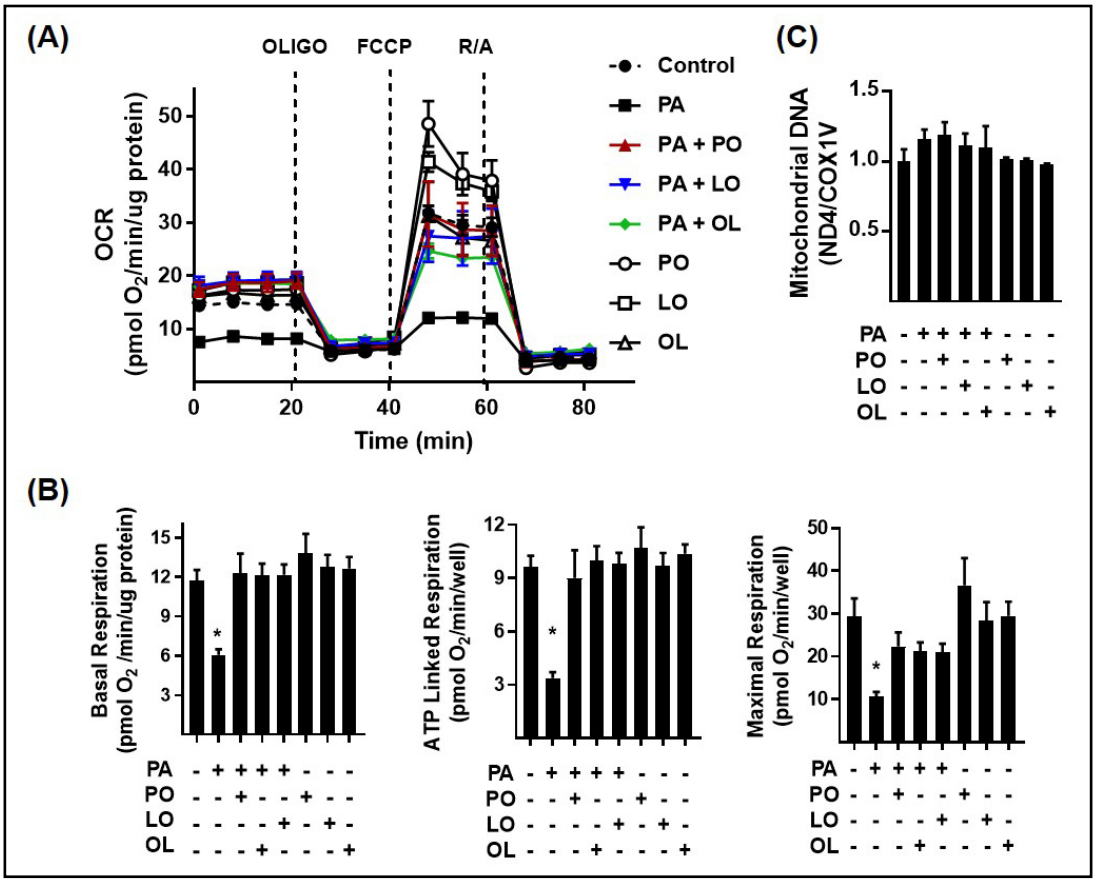

Fig. 4. Effect of palmitate and/or unsaturated fatty acids on mitochondrial respiratory function. L6 myotubes were incubated for 16 h in media containing D-glucose (5 mM) supplemented with or without palmitate (PA, 0.4 mM) or unsaturated fatty acids palmitoleate (PO, C16:1), Oleate (OL, C18:1) or linoleate (LO, C18:2) at 0.4 mM as indicated prior to analysis of real-time cellular respiration using a Seahorse XF24 analyser. Oligomycin (1 μM), FCCP (1 μM) and a rotenone (1 μM)/antimycin-A (2 μM) mix were added at times indicated by the dotted lines. (A) shows a representative readout of oxygen consumption rate (OCR) from a single experiment with each data point representing the mean ± SD of a triplicate measurement. (B) The graphical data shows basal respiration, ATP-linked respiration and maximal respiration (OCR after FCCP stimulation). (C) Mitochondrial DNA quantification by qPCR. Data in (B) and (C) are mean ± SEM from 5 and 3 independent experiments, respectively. The asterisk indicates a significant change ($P<0.05$) to the control condition (lacking any fatty acid additions).

Mono- and poly-unsaturated fatty acids prevent the loss of mitochondrial proteins induced by palmitate

In myotubes, PA has been shown to induce deleterious changes in the abundance of proteins linked to regulation of mitochondrial biogenesis and respiratory function and these changes can be countered by inhibiting the associated increase in proinflammatory NFkB signalling caused by the SFA [21]. Since MUFAs and PUFAs can repress PA-induced NFkB signalling (Fig. 2, [34]) we subsequently assessed whether the ability of PO, OL and LO to restrain PA-induced disturbances in respiratory function involved mitigating changes in proteins that impact mitochondrial biology. Fig. 5 shows that PA caused a significant decline in PGC1α, a transcriptional coactivator that plays a key role in regulating mitochondrial biogenesis and function, as well that of succinate dehydrogenase (SDHA), mitochondrial ADP-ATP translocase (ANT1) and uncoupling protein 3 (UCP3) that all have crucial roles in OXPHOS. In addition, the abundance of NRF1, which has been linked to the transcriptional control of numerous genes involved in mitochondrial function was reduced by ~70%, whereas that of NRF2, a protein involved in regulating oxidative stress-induced gene expression was only modestly affected by PA but whose abundance was elevated in myotubes incubated with PO, OL or LO. Fig. 5 also shows that the abundance of two key anti-oxidant enzymes, MnSOD2 and catalase, were elevated in myotubes by PA, but, consistent with our recent work [21], PA did not induce any notable changes in COX4.1 or TFAM, a component of the mitochondrial transcription initiation complex. Notably, however, the changes induced in the protein abundance of PGC1α, SDHA, ANT1, UCP3, NRF1, MnSOD2 and catalase by PA oversupply were antagonised in myotubes that were co-incubated with PO, OL and LO.

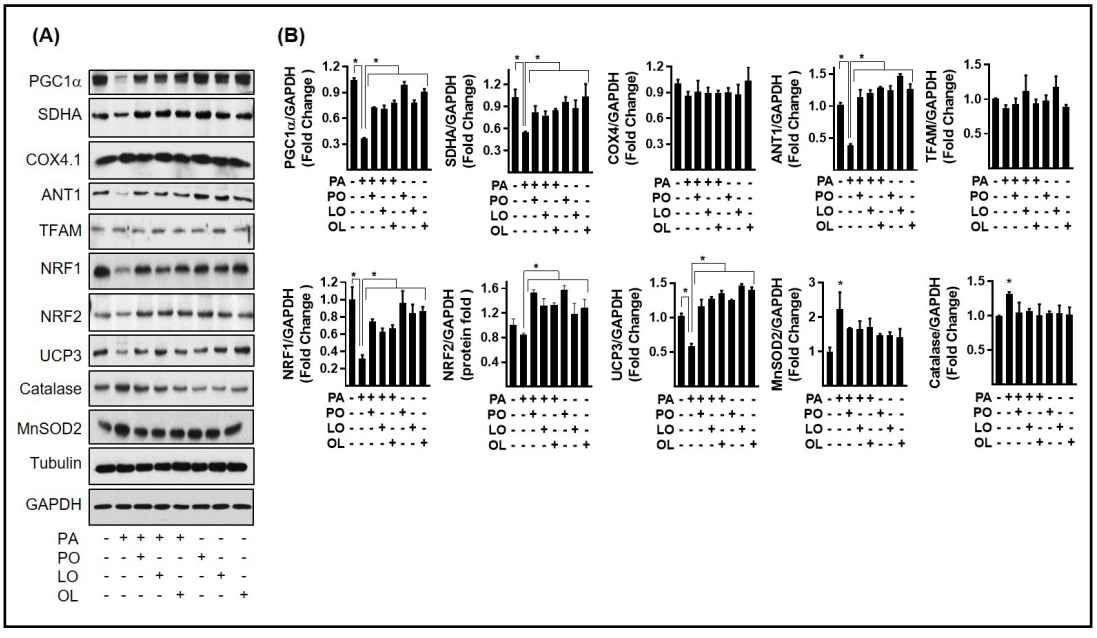

Fig. 5. Effect of palmitate and/or unsaturated fatty acids on the abundance of proteins implicated in the regulation of mitochondrial function. L6 myotubes were incubated for 16 h in media containing D-glucose (5 mM) supplemented with or without palmitate (PA, 0.4 mM) or unsaturated fatty acids palmitoleate (PO, C16:1), Oleate (OL, C18:1) or linoleate (LO, C18:2) at 0.4 mM as indicated prior to cell lysis and (A) immunoblot and (B) quantitative analysis of PGC1α, SDHA, COX4.1, ANT1, TFAM, NRF1, NRF2, UCP3, Catalase, and MnSOD2. Data in (B) are presented as mean ± SEM from three or four separate experiments (one sample/condition/experiment). The asterisk indicates a significant change ($P<0.05$) to the control condition (lacking any fatty acid additions) or between the indicated bars.

Effects of fatty acid provision on mitochondrial ROS generation and mitochondrial membrane potential

Mitochondrial respiration represents a primary site of ROS generation because of oxygen being reduced by electrons "leaking" out from within the ETC. ROS generation is elevated in skeletal muscle cells under conditions when supply of respiratory fuel exceeds cellular energy demand [21] and, as such, this has been linked to increased mitochondrial fragmentation and mitochondrial depolarisation [21, 40]. We consequently sought to address the impact of fatty acid provision on ROS and mitochondrial membrane potential within L6 myotubes. For analysis of superoxide we utilised MitoSox, a fluorogenic probe whose targeted accumulation and oxidation by superoxide in mitochondria generates red fluorescence that can be visualised by live cell imaging. Fig. 6A shows that myotubes treated with 0.4 mM PA for 16 h exhibit a 2-fold increase in superoxide, which was countered by co-incubating myotubes with PO, OL and LO in a dose-dependent manner. Of these fatty acids, PO was the most potent in suppressing PA-induced superoxide generation although none, by themselves, invoked any significant change in superoxide content in myotubes. For analysis of hydrogen

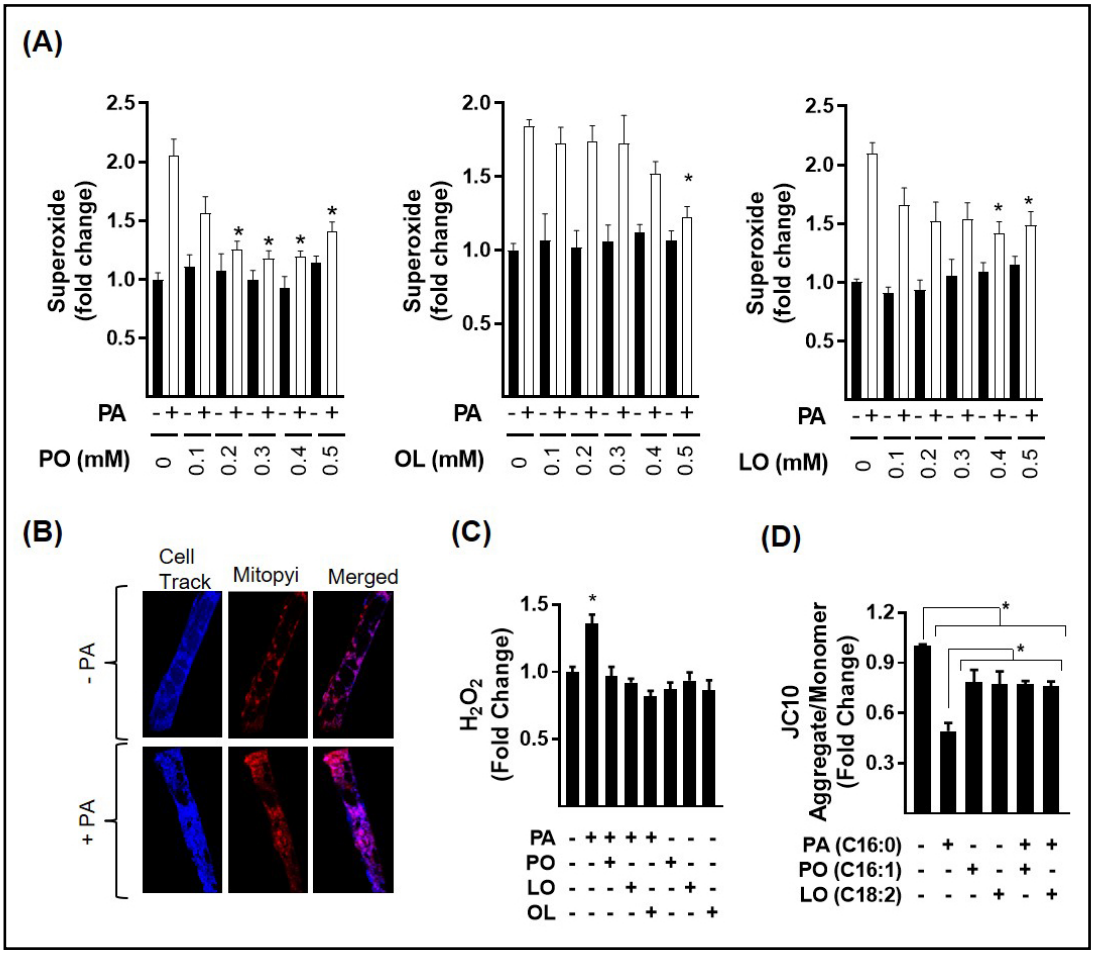

Fig. 6. Effect of palmitate and/or unsaturated fatty acids on mitochondrial ROS production. L6 myotubes were incubated for 16 h in media containing D-glucose (5 mM) supplemented with or without palmitate (PA, 0.4 mM) or unsaturated fatty acids palmitoleate (PO, C16:1), Oleate (OL, C18:1) or linoleate (LO, C18:2) at the concentrations indicated prior to analysis of (A) superoxide production (five measurements/condition/experiment); (B and C) H_2O_2 production and (D) mitochondrial membrane potential using spectral analysis to monitor JC-10 aggregate: monomer content. Data are presented as mean ± SEM from a minimum of four separate experiments. The asterisk indicates a significant change ($P<0.05$) to the control condition (lacking any fatty acid additions) or between the indicated bars.

peroxide (H_2O_2) under live cell conditions, L6 myotubes were incubated with MitoPYI (a mitochondrial specific florescent H_2O_2 probe). Fig. 6B depicts representative live cell images of myotubes incubated in the absence or presence of PA revealing heightened MitoPYI fluorescence in PA-treated myotubes that were costained blue with Cell Tracker dye. Quantification of MitoPYI fluorescence indicated that this PA-induced increase in mitochondrial H_2O_2 was ~40% and was blunted in myotubes upon coincubation with PO, OL or LO (Fig. 6C). Again, these fatty acids alone had no discernible effect on H_2O_2 content in myotubes.

Mitochondrial membrane depolarization is associated with increased ROS production and serves as an indicator of mitochondrial dysfunction. In separate experiments we monitored the effects of SFA, MUFA and PUFA provision to myotubes on the aggregate to monomer ratio of a potentiometric fluorescent dye, JC10, as readout of mitochondrial potential. In healthy cells, JC10 accumulates within mitochondria and forms red fluorescent aggregates, whereas depolarised mitochondria allow the dye to leak out in its monomeric form and stain cells green. Fig. 6D shows that whilst a sustained 16h incubation of myotubes with 0.4 mM PO or LO induced a modest reduction in the JC10 aggregate/monomer ratio relative to untreated cells, PA has a much more pronounced effect causing a greater depolarisation of the mitochondrial membrane potential. This PA-induced mitochondrial depolarisation was partially mitigated in myotubes that had been coincubated with PO and LO.

Discussion

Recent work from our group has demonstrated that the proinflammatory drive that is instituted in skeletal muscle cells in response sustained over supply of SFAs, such as PA, is mechanistically linked to increases in mitochondrial redox stress and disturbances in mitochondrial form and function [21]. In the current study we show that these fatty acid-induced changes in mitochondrial biology are not evident when myotubes are incubated with equivalent concentrations of laurate (LA), a medium chain (C12:0) SFA, or when treated with long chain mono- and poly-unsaturated fatty acids (PO, C16:1; OL, C18:1; LO, C18:2). Strikingly, unlike PA or stearate (another long chain (C18:0) SFA), we show that PO, OL and LO do not promote an increase in proinflammatory NFkB signalling and, significantly, that they not only antagonise the proinflammatory action of PA, but also mitigate the pathogenic shift in mitochondrial morphology, bioenergetics and redox status induced by this SFA.

Previous studies have shown that the increase in proinflammatory NFkB signalling associated with oversupply of PA may be linked with its ability to engage with and activate toll-like receptors [41] or *via* intracellular stimulation of kinases such as PKCΘ [26], JNK and ERK [9] that act as upstream activators of the IKK-NFkB axis. While activation of NFkB signalling in this context stimulates expression of genes encoding proinflammatory cytokines (e.g. IL-6 and TNFα) that may contribute to development of insulin resistance [42], there is also increasing recognition that heightened NFkB activation represses expression of genes with important roles in mitochondrial biology such as the transcriptional coactivator, PGC1α [43] and the ADP/ATP translocase, ANT1 [44]. Repression of the former would affect expression of PGC1α target genes such as NRF1 and NRF2 [45, 46] that, in turn, will impact negatively upon expression of their gene targets including UCP3 and respiratory proteins such as SDHA [47, 48], whereas repression of the latter would compromise production and transfer of mitochondrial ATP to the cytoplasm [44]. Consistent with these molecular links, our data indicate that PA induces a reduction in the protein abundance of PGC1α, ANT1, NRF1, UCP3 and SDHA that notably are associated with a significant decline in mitochondrial respiratory function. We have previously shown that the PA-induced loss of these proteins and the associated reduction in respiratory capacity can be blunted upon inhibition of NFkB-signalling in muscle cells [21] and, as illustrated here, also when myotubes were coincubated with either PO and OL (MUFAs) or LO (a PUFA). We contest that the ability of these fatty acids to restrain PA-induced mitochondrial dysfunction is most likely linked to their anti-inflammatory action as judged by their capacity to repress IkBα loss and IL6 gene

expression by PA. Precisely how they antagonise PA-induced NFkB signalling remains poorly resolved, but previous work has suggested that MUFAs (PO and OL) not only induce greater partitioning of PA into neutral triglyceride but stimulate mitochondrial fatty acid oxidation [26, 34] and that, by doing so, this may reduce its channelling into fatty acid derivatives such as DAG and ceramides that can induce NFkB signalling *via* activation of stress kinases [9, 26]. The ability of OL to increase fatty acid oxidation has been linked to activation of the cAMP/protein kinase A (PKA) pathway, which stimulates the SIRT1-PGC1α transcriptional complex to upregulate genes supporting fatty acid oxidation in myotubes [49]. The notion that this increase in fatty acid oxidation then helps off-set the proinflammatory potential of PA, and by extension its capacity to promote mitochondrial dysfunction, is supported by data showing that if uptake and oxidation of fatty acids by mitochondria is suppressed using etomoxir then the ability of OL and PO to restrain PA-induced NFkB signalling is markedly reduced in C2C12 and L6 myotubes [26, 34]. Furthermore, inhibition of PKA not only attenuates the OL-induced increase in fatty acid oxidation but curtails the capacity of this MUFA to rescue PGC1α loss in PA-treated myotubes, which is widely regarded as being important for maintaining mitochondrial homeostasis [26, 49].

A key observation in the present study was the differential effect that acyl chain length and saturation have upon mitochondrial morphology. In terminally differentiated L6 myotubes that have not been subjected to fatty acid treatments the mitochondrial network is predominantly (~80%) elongated/tubular in nature, which is considered more "healthy" and "efficient" than that seen in myotubes treated with PA in which mitochondria are primarily small rounded punctate structures. This shift to a more fragmented morphology was not seen in myotubes treated with LA (C12:0), PO, OL or LO, but, compared to PA, was further exacerbated in L6 myotubes incubated with stearate (C18:0) suggesting that saturation and increased acyl chain length are important fatty acid characteristics driving mitochondrial fragmentation that, interestingly, also correlate with their capacity to activate proinflammatory NFkB signalling. Mitochondrial morphology is critically dependent on the relative expression/activity of proteins that on the one hand support mitochondrial fusion (mitofusins (MFN1 and 2) and Opa1) and on the other those promoting mitochondrial fission (Drp1 and Fis1). We could not detect any meaningful changes in the total myocellular abundance of Opa1 or Drp1 in L6 myotubes in response to PA overloading (data not shown) but did observe a significant reduction in MFN2. MFN2 expression has been shown to be rapidly downregulated *in vivo* in response to high fat feeding and its expression is also reduced by proinflammatory cytokines, lipid availability, and glucocorticoids [50, 51]. In skeletal muscle, PGC1α has been shown to stimulate expression of the Mfn2 gene promoter [52] and given that PA represses PGC1α in our myotubes this may help account for the observed reduction in MFN2. Consistent with the ability of PO, OL and LO to restrain PGC1α loss in PA-treated myotubes, these fatty acids also antagonise the PA-induced loss of MFN2, which may then help facilitate retention of an elongated/tubular mitochondrial network that also exhibits greater respiratory competency. It is, however, noteworthy that similar studies in C2C12 myoblasts in which PA also induces mitochondrial fragmentation did not report any change in MFN2 abundance but did observe increases in both Drp1 and Fis1 [53]. The reasons for this discrepancy are unclear but may reflect differences that are either cell-type (murine C2C12 versus rat L6) and/or differentiation (myoblast versus myotube) dependent. In any event, the PA-induced loss of MFN2 in L6 myotubes or the increase in Drp1/Fis1 in C2C12 myoblasts would result in a dynamic shift towards greater mitochondrial fission that correlates with reduced mitochondrial respiratory capacity in both experimental systems.

Increased oxidative stress is also an important regulator of mitochondrial morphology and has been shown to induce recruitment of Drp1 to mitochondria where it initiates mitochondrial fragmentation that, importantly, can be restrained by ROS scavenging molecules [54]. While we see no overall change in cellular Drp1 content in PA-treated myotubes we have previously noted that PA induces a modest increase in mitochondrial associated Drp1 when there is backdrop of heightened mitochondrial ROS production [21]. Under these circumstances, fragmentation of the mitochondrial network caused by PA can be halted by Mi-

totempo, a mitochondrial targeted anti-oxidant, thus further underscoring the crucial role that ROS play in regulating mitochondrial dynamics [21]. The current findings extend on these observations by demonstrating that whilst PA induces a significant increase in both mitochondrial superoxide and hydrogen peroxide this increase is not evident in myotubes treated with PO, OL or LO and, significantly, that these fatty acids blunt PA driven ROS generation. This anti-oxidant effect is not unprecedented as studies in C2C12 myotubes examining the tight coupling between a rise in mitochondrial ROS and muscle atrophy have shown that OL not only antagonises ROS production, but negates the expression of genes involved in muscle atrophy (e.g. myostatin and atrogin1) and the decline in myotube width that are induced by chronic PA treatment [33]. Precisely how availability of OL modifies myotube redox status under these circumstances is unclear but it may be linked to regulation of Nrf2, a key transcription factor involved in mediating anti-oxidant responses *via* modulation of NADPH:quinone oxidoreductase 1 and Glutathione S-Transferase gene expression [55, 56]. Our data indicate that PO, OL and LO all elevate the abundance of this transcription factor relative to that seen in myotubes chronically treated with PA which, by contrast, exhibit a modest reduction in Nrf2. Previous studies could not demonstrate any OL-dependent increase in Nrf2 gene expression in PA-treated myotubes [33] thus potentially raising the possibility that the increase in Nrf2 we see following treatment with our test MUFAs and PUFA might be linked to increased protein stability, possibly by inhibiting its normal degradation *via* the ubiquitin proteasome pathway [57]. Whether Nrf2 is stabilised by such a mechanism and contributes to the antioxidant response of PO, OL and LO is currently unknown but testing this possibility may prove instructive in understanding the differential effect that saturated and unsaturated fatty acids have on cellular redox status.

Mitochondrial integrity is also critically influenced by cardiolpin, a phospholipid that is almost exclusively synthesised and located within the inner mitochondrial membrane (IMM) where it impacts on numerous mitochondrial processes, including cristae formation and regulating the spatial organisation of IMM proteins, such as those constituting the respiratory chain and those involved in synthesis and membrane exchange of ATP [58, 59]. Although the current study did not assay cardiolipin content in myotubes, there is evidence in the literature showing that chronic exposure of cells to PA results in cardiolipin loss [60]. This decline in cardiolipin is associated with reduced mitochondrial integrity as judged by depolarisation of the mitochondrial membrane and release of cytochrome c, which, notably, was not seen in cells incubated with OL or LO [60]. Significantly, cardiolipin is a tetra-acyl phospholipid in which the fatty acid chains are highly specific being comprised primarily of 18C unsaturated acyl chains (e.g. LO, 18:2) [58]. It is plausible that in cells chronically exposed to PA that cardiolipin shifts away from the 18:2 rich species or, alternatively, is rendered more susceptible to peroxidation and degradation by ROS [61], whose generation would be greatly elevated in cells subject to PA oversupply. Since both OL and LO counter PA-induced increases in ROS as well as the associated disturbances in mitochondrial integrity and respiratory capacity it is plausible that these metabolic benefits may partly rely upon repressing mitochondrial cardiolipin loss by PA.

We, and others, have previously argued that sustained fuel overloading of muscle cells under circumstances when there is no associated increase in energy demand will ultimately culminate in mitochondrial insufficiency that will most likely exacerbate the effects of heightened ROS production and lipotoxicity on key cellular functions, such as those regulated by insulin [21, 31, 62-64]. If this supposition is correct, then how is it that co-supplementation of PO, OL or LO negates mitochondrial dysfunction induced by PA when there is unlikely to be any change in energy demand? One potential explanation might involve increased uncoupling across the IMM which would stimulate fuel oxidation without generating ATP [65]. Fatty acids have long been known to possess protonophoric activity and cause mild uncoupling by interacting with proteins that can transfer fatty acid anions across the IMM, such as ANT-1 [66, 67]. The presence of UCP3 may also contribute to uncoupling of OXPHOS in muscle cells, but this UCP family member may also function to remove fatty acid anions that have accumulated at the matrix-facing membrane [68]. Whilst only fatty acids

that have been activated to their acyl CoA derivatives are oxidised in the mitochondria, it has been suggested that in response to fatty acid over supply some fatty acyl CoA molecules are deactivated by mitochondrial thioesterase to help liberate CoA for use in other mitochondrial reactions [69]. This deactivation generates fatty acid anions that cannot be oxidised. Furthermore, under these circumstances, fatty acids that may not have been activated in the cytosol might "flip-flop" across the mitochondrial membrane and partition into the mitochondrial matrix where they can be deprotonated to their anion form. The fatty acid anions generated by these mechanisms are very susceptible to peroxidation and their accumulation in the matrix is potentially deleterious for mitochondrial function. Consequently, the export of fatty acid anions from the matrix *via* UCP3 will not only help sustain an optimal flux for fatty acid oxidation, but also help lower the membrane potential and limit ROS generation in myotubes [68]. The observation that the MUFAs and PUFA used in our study induce a partial depolarisation of the mitochondrial membrane and mitigate mitochondrial ROS production (Fig. 6) in PA-overloaded myotubes is fully consistent with this latter proposition. Our findings also indicate that such changes, will themselves, be dependent upon these fatty acids restraining the PA-induced loss of proteins that critically support both mitochondrial form and function (e.g. MFN2, PGC1α, SDHA, NRF1, ANT1, UCP3 etc).

Conclusion

In summary, the present study provides evidence that saturated and unsaturated fatty acids exert distinct effects upon mitochondrial morphology and respiratory function in skeletal muscle cells *in vitro*. Specifically, our data indicate that unsaturated fatty acids confer protection against cellular inflammation, increased ROS generation and disturbances in mitochondrial homeostasis induced by the sustained over supply of PA. Our data signal that such benefits are unlikely to be a consequence of simple uptake competition in which PA is excluded from muscle cells by unsaturated fatty acids given that we found that OL enhanced PA uptake in our hands. This observation is consistent with work showing that OL dose-dependently increases oxidation of radio-labelled [^{14}C]-palmitate to [^{14}C]-CO_2 in C2C12 myotubes [70], which may be linked to the stimulatory effect that OL has on expression of genes involved in fatty acid oxidation in skeletal muscle both *in vitro* and *in vivo* [49]. Whether an increase in fatty acid oxidation alone can explain the observed increase in PA uptake that we see with OL or if this also involves upregulation cell surface fatty acid transporters is currently unknown, but testing these possibilities represent important investigative goals of future work. Whilst we remain mindful of the limitations of our *in vitro* cell based model we believe our data may have important implications for understanding the impact of dietary fat composition on cell/tissue function. Previous studies have, for example, pointed to the potential health and therapeutic benefits of unsaturated fatty acids in the treatment of metabolic diseases such as diabetes [71] as well as cardiovascular [72] and neurodegenerative [73] conditions. Our observations would suggest that such benefits may be critically dependent upon preserving cellular energy homeostasis and might be achievable *in vivo* if energy intake from dietary fat was weighted in favour of MUFAs and PUFAs, rather than SFAs. Future long-term dietary intervention studies comparing how modifying fat composition impacts upon inflammatory tone, metabolic profiles and energy status within tissues such as skeletal muscle may therefore prove extremely instructive in establishing the translational value of some of the findings reported here.

Abbreviations

ANT-1 (Adenine nucleotide translocase type 1); IKBα (Inhibitor of Nuclear factor Kappa-B); IL-6 (Interleukin-6); LA (Laurate); LO (Linoleate); MFN2 (Mitofusin 2); MUFA (Monounsaturated Fatty Acid); NRF1 (Nuclear Respiratory Factor 1); NRF2 (Nuclear Factor Erythroid

2); OL (Oleate); PGC1α (Peroxisome proliferator-activated receptor gamma coactivator 1-alpha); PO (Palmitoleate); PUFA (Polyunsaturated Fatty Acid); ROS (Reactive Oxygen Species); SDHA (Succinate Dehydrogenase); SFA (Saturated Fatty Acid); SOD2 (Superoxide Dismutase 2); ST (Stearate); UCP3 (Uncoupling protein 3).

Acknowledgements

We thank Calum Fordyce for participation in some of the experiments reported. We would like to thank members of Hundal laboratory for their comments on the manuscript.

All authors have read and approved the final manuscript submitted for publication.

Author Contributions

RBN performed the experiments, analysed the data and contributed to drafting and editing the manuscript. DSS performed experimental work. HSH directed the research, wrote and edited the manuscript.

Funding Sources

The studies reported herein were supported by Diabetes UK and the BBSRC.

Statement of Ethics

The authors have no ethical conflicts to disclose.

Disclosure Statement

The authors have no conflicts of interest to declare.

References

1 Boden G: Fatty acid-induced inflammation and insulin resistance in skeletal muscle and liver. Curr Diab Rep 2006;6:177-181.
2 Green CJ, Pedersen M, Pedersen BK, Scheele C: Elevated NF-kappaB activation is conserved in human myocytes cultured from obese type 2 diabetic patients and attenuated by AMP-activated protein kinase. Diabetes 2011;60:2810-2819.
3 Boden G, Shulman GI: Free fatty acids in obesity and type 2 diabetes: defining their role in the development of insulin resistance and beta-cell dysfunction. Eur J Clin Invest 2002;32:14-23.
4 Leyton J, Drury PJ, Crawford MA: Differential oxidation of saturated and unsaturated fatty acids *in vivo* in the rat. Br J Nutr 1987;57:383-393.
5 DeLany JP, Windhauser MM, Champagne CM, Bray GA: Differential oxidation of individual dietary fatty acids in humans. Am J Clin Nutr 2000;72:905-911.
6 Gaster M, Rustan AC, Beck-Nielsen H: Differential utilization of saturated palmitate and unsaturated oleate: evidence from cultured myotubes. Diabetes 2005;54:648-656.
7 Hariri N, Gougeon R, Thibault L: A highly saturated fat-rich diet is more obesogenic than diets with lower saturated fat content. Nutr Res 2010;30:632-643.
8 Koves TR, Ussher JR, Noland RC, Slentz D, Mosedale M, Ilkayeva O, et al.: Mitochondrial overload and incomplete fatty acid oxidation contribute to skeletal muscle insulin resistance. Cell Metab 2008;7:45-56.
9 Green CJ, Macrae K, Fogarty S, Hardie DG, Sakamoto K, Hundal HS: Counter-modulation of fatty acid-induced pro-inflammatory nuclear factor kappaB signalling in rat skeletal muscle cells by AMP-activated protein kinase. Biochem J 2011;435:463-474.
10 Coll T, Alvarez-Guardia D, Barroso E, Gomez-Foix AM, Palomer X, Laguna JC, et al.: Activation of peroxisome proliferator-activated receptor-{delta} by GW501516 prevents fatty acid-induced nuclear factor-{kappa}B activation and insulin resistance in skeletal muscle cells. Endocrinology 2010;151:1560-1569.

11 Rutkowsky JM, Knotts TA, Ono-Moore KD, McCoin CS, Huang S, Schneider D, et al.: Acylcarnitines activate proinflammatory signaling pathways. Am J Physiol Endocrinol Metab 2014;306:E1378-E1387.
12 Powell DJ, Turban S, Gray A, Hajduch E, Hundal HS: Intracellular ceramide synthesis and protein kinase Czeta activation play an essential role in palmitate-induced insulin resistance in rat L6 skeletal muscle cells. Biochem J 2004;382:619-629.
13 Chavez JA, Knotts TA, Wang LP, Li G, Dobrowsky RT, Florant GL, et al.: A role for ceramide, but not diacylglycerol, in the antagonism of insulin signal transduction by saturated fatty acids. J Biol Chem 2003;278:10297-10303.
14 Yu C, Chen Y, Cline GW, Zhang D, Zong H, Wang Y, et al.: Mechanism by which fatty acids inhibit insulin activation of insulin receptor substrate-1 (IRS-1)-associated phosphatidylinositol 3-kinase activity in muscle. J Biol Chem 2002;277:50230-50236.
15 Powell DJ, Hajduch E, Kular G, Hundal HS: Ceramide Disables 3-Phosphoinositide Binding to the Pleckstrin Homology Domain of Protein Kinase B (PKB)/Akt by a PKCzeta-Dependent Mechanism. Mol Cell Biol 2003;23:7794-7808.
16 Ritov VB, Menshikova EV, He J, Ferrell RE, Goodpaster BH, Kelley DE: Deficiency of subsarcolemmal mitochondria in obesity and type 2 diabetes. Diabetes 2005;54:8-14.
17 Putti R, Migliaccio V, Sica R, Lionetti L: Skeletal Muscle Mitochondrial Bioenergetics and Morphology in High Fat Diet Induced Obesity and Insulin Resistance: Focus on Dietary Fat Source. Front Physiol 2015;6:426.
18 Kelley DE, He J, Menshikova EV, Ritov VB: Dysfunction of mitochondria in human skeletal muscle in type 2 diabetes. Diabetes 2002;51:2944-2950.
19 Holloszy JO: "Deficiency" of mitochondria in muscle does not cause insulin resistance. Diabetes 2013;62:1036-1040.
20 Goodpaster BH: Mitochondrial deficiency is associated with insulin resistance. Diabetes 2013;62:1032-1035.
21 Nisr RB, Shah DS, Ganley IG, Hundal HS: Proinflammatory NFkB signalling promotes mitochondrial dysfunction in skeletal muscle in response to cellular fuel overloading. Cell Mol Life Sci 2019;76:4887-4904.
22 Yuzefovych LV, Solodushko VA, Wilson GL, Rachek LI: Protection from palmitate-induced mitochondrial DNA damage prevents from mitochondrial oxidative stress, mitochondrial dysfunction, apoptosis, and impaired insulin signaling in rat L6 skeletal muscle cells. Endocrinology 2012;153:92-100.
23 Dimopoulos N, Watson M, Sakamoto K, Hundal HS: Differential effects of palmitate and palmitoleate on insulin action and glucose utilization in rat L6 skeletal muscle cells. Biochem J 2006;399:473-481.
24 Cao H, Gerhold K, Mayers JR, Wiest MM, Watkins SM, Hotamisligil GS: Identification of a lipokine, a lipid hormone linking adipose tissue to systemic metabolism. Cell 2008;134:933-944.
25 Gillingham LG, Harris-Janz S, Jones PJ: Dietary monounsaturated fatty acids are protective against metabolic syndrome and cardiovascular disease risk factors. Lipids 2011;46:209-228.
26 Coll T, Eyre E, Rodriguez-Calvo R, Palomer X, Sanchez RM, Merlos M, et al.: Oleate reverses palmitate-induced insulin resistance and inflammation in skeletal muscle cells. J Biol Chem 2008;283:11107-11116.
27 Peng G, Li L, Liu Y, Pu J, Zhang S, Yu J, et al.: Oleate blocks palmitate-induced abnormal lipid distribution, endoplasmic reticulum expansion and stress, and insulin resistance in skeletal muscle. Endocrinology 2011;152:2206-2218.
28 Vessby B, Unsitupa M, Hermansen K, Riccardi G, Rivellese AA, Tapsell LC, et al.: Substituting dietary saturated for monounsaturated fat impairs insulin sensitivity in healthy men and women: The KANWU Study. Diabetologia 2001;44:312-319.
29 Cruz MM, Lopes AB, Crisma AR, de Sa RCC, Kuwabara WMT, Curi R, et al.: Palmitoleic acid (16:1n7) increases oxygen consumption, fatty acid oxidation and ATP content in white adipocytes. Lipids Health Dis 2018;17:55.
30 Staiger H, Staiger K, Haas C, Weisser M, Machicao F, Haring HU: Fatty acid-induced differential regulation of the genes encoding peroxisome proliferator-activated receptor-gamma coactivator-1alpha and -1beta in human skeletal muscle cells that have been differentiated *in vitro*. Diabetologia 2005;48:2115-2118.
31 Nisr RB, Affourtit C: Palmitate-induced changes in energy demand cause reallocation of ATP supply in rat and human skeletal muscle cells. Biochim Biophys Acta 2016;1857:1403–1411.

32 Yuzefovych L, Wilson G, Rachek L: Different effects of oleate vs. palmitate on mitochondrial function, apoptosis, and insulin signaling in L6 skeletal muscle cells: role of oxidative stress. Am J Physiol Endocrinol Metab 2010;299:E1096-E1105.
33 Lee H, Lim JY, Choi SJ: Oleate Prevents Palmitate-Induced Atrophy via Modulation of Mitochondrial ROS Production in Skeletal Myotubes. Oxid Med Cell Longev 2017;2017:2739721.
34 Macrae K, Stretton C, Lipina C, Blachnio-Zabielska A, Baranowski M, Gorski J, et al.: Defining the role of DAG, mitochondrial function and lipid deposition in palmitate-induced proinflammatory signalling and its counter-modulation by palmitoleate. J Lipid Res 2013;54:2366-2378.
35 Cheon HG, Cho YS: Protection of palmitic acid-mediated lipotoxicity by arachidonic acid via channeling of palmitic acid into triglycerides in C2C12. J Biomed Sci 2014;21:13.
36 Cavaliere G, Trinchese G, Bergamo P, De Filippo C, Mattace Raso G, Gifuni G, et al.: Polyunsaturated Fatty Acids Attenuate Diet Induced Obesity and Insulin Resistance, Modulating Mitochondrial Respiratory Uncoupling in Rat Skeletal Muscle. PLoS One 2016;11:e0149033.
37 Hajduch E, Alessi DR, Hemmings BA, Hundal HS: Constitutive activation of Protein Kinase Ba (PKBa) by membrane targeting promotes glucose and System A amino acid transport, protein synthesis and GSK3 inactivation in L6 muscle cells. Diabetes 1998;47:1006-1013.
38 Stierwalt HD, Ehrlicher SE, Bergman BC, Robinson MM, Newsom SA: Insulin-stimulated Rac1-GTP binding is not impaired by palmitate treatment in L6 myotubes. Physiol Rep 2018;6:e13956.
39 Yoon JH, Kim D, Jang JH, Ghim J, Park S, Song P, et al.: Proteomic analysis of the palmitate-induced myotube secretome reveals involvement of the annexin A1-formyl peptide receptor 2 (FPR2) pathway in insulin resistance. Mol Cell Proteomics 2015;14:882-892.
40 Iqbal S, Ostojic O, Singh K, Joseph AM, Hood DA: Expression of mitochondrial fission and fusion regulatory proteins in skeletal muscle during chronic use and disuse. Muscle Nerve 2013;48:963-970.
41 Senn JJ: Toll-like receptor-2 is essential for the development of palmitate-induced insulin resistance in myotubes. J Biol Chem 2006;281:26865-26875.
42 de Alvaro C, Teruel T, Hernandez R, Lorenzo M: Tumor necrosis factor alpha produces insulin resistance in skeletal muscle by activation of inhibitor kappaB kinase in a p38 MAPK-dependent manner. J Biol Chem 2004;279:17070-17078.
43 Alvarez-Guardia D, Palomer X, Coll T, Serrano L, Rodriguez-Calvo R, Davidson MM, et al.: PPARbeta/delta activation blocks lipid-induced inflammatory pathways in mouse heart and human cardiac cells. Biochim Biophys Acta 2011;1811:59-67.
44 Zhang C, Jiang H, Wang P, Liu H, Sun X: Transcription factor NF-kappa B represses ANT1 transcription and leads to mitochondrial dysfunctions. Sci Rep 2017;7:44708.
45 Wu Z, Puigserver P, Andersson U, Zhang C, Adelmant G, Mootha V, et al.: Mechanisms controlling mitochondrial biogenesis and respiration through the thermogenic coactivator PGC-1. Cell 1999;98:115-124.
46 Mootha VK, Lindgren CM, Eriksson KF, Subramanian A, Sihag S, Lehar J, et al.: PGC-1alpha-responsive genes involved in oxidative phosphorylation are coordinately downregulated in human diabetes. Nat Genet 2003;34:267-273.
47 Lopez-Bernardo E, Anedda A, Sanchez-Perez P, Acosta-Iborra B, Cadenas S: 4-Hydroxynonenal induces Nrf2-mediated UCP3 upregulation in mouse cardiomyocytes. Free Radic Biol Med 2015;88:427-438.
48 Au HC, Scheffler IE: Promoter analysis of the human succinate dehydrogenase iron-protein gene--both nuclear respiratory factors NRF-1 and NRF-2 are required. Eur J Biochem 1998;251:164-174.
49 Lim JH, Gerhart-Hines Z, Dominy JE, Lee Y, Kim S, Tabata M, et al.: Oleic acid stimulates complete oxidation of fatty acids through protein kinase A-dependent activation of SIRT1-PGC1alpha complex. J Biol Chem 2013;288:7117-7126.
50 Mancini G, Pirruccio K, Yang X, Bluher M, Rodeheffer M, Horvath TL: Mitofusin 2 in Mature Adipocytes Controls Adiposity and Body Weight. Cell Rep 2019;27:648.
51 Zorzano A, Hernández-Alvarez MI, Sebastián D, Muñoz JP: Mitofusin 2 as a driver that controls energy metabolism and insulin signaling. Antioxid Redox Signal 2015;22:1020-1031.
52 Soriano FX, Liesa M, Bach D, Chan DC, Palacin M, Zorzano A: Evidence for a mitochondrial regulatory pathway defined by peroxisome proliferator-activated receptor-gamma coactivator-1 alpha, estrogen-related receptor-alpha, and mitofusin 2. Diabetes 2006;55:1783-1791.

53 Jheng HF, Tsai PJ, Guo SM, Kuo LH, Chang CS, Su IJ, et al.: Mitochondrial fission contributes to mitochondrial dysfunction and insulin resistance in skeletal muscle. Mol Cell Biol 2012;32:309-319.
54 Wu S, Zhou F, Zhang Z, Xing D: Mitochondrial oxidative stress causes mitochondrial fragmentation via differential modulation of mitochondrial fission-fusion proteins. FEBS J 2011;278:941-954.
55 Ahmed SMU, Luo L, Namani A, Wang XJ, Tang X: Nrf2 signaling pathway: Pivotal roles in inflammation. Biochim Biophys Acta Mol Basis Dis 2017;1863:585-597.
56 Nguyen T, Nioi P, Pickett CB: The Nrf2-antioxidant response element signaling pathway and its activation by oxidative stress. J Biol Chem 2009;284:13291-13295.
57 Tebay LE, Robertson H, Durant ST, Vitale SR, Penning TM, Dinkova-Kostova AT, et al.: Mechanisms of activation of the transcription factor Nrf2 by redox stressors, nutrient cues, and energy status and the pathways through which it attenuates degenerative disease. Free Radic Biol Med 2015;88:108-146.
58 Chicco AJ, Sparagna GC: Role of cardiolipin alterations in mitochondrial dysfunction and disease. Am J Physiol Cell Physiol 2007;292:C33-C44.
59 Ban T, Ishihara T, Kohno H, Saita S, Ichimura A, Maenaka K, et al.: Molecular basis of selective mitochondrial fusion by heterotypic action between OPA1 and cardiolipin. Nat Cell Biol 2017;19:856-863.
60 Buratta M, Castigli E, Sciaccaluga M, Pellegrino RM, Spinozzi F, Roberti R, et al.: Loss of cardiolipin in palmitate-treated GL15 glioblastoma cells favors cytochrome c release from mitochondria leading to apoptosis. J Neurochem 2008;105:1019-1031.
61 Wiswedel I, Gardemann A, Storch A, Peter D, Schild L: Degradation of phospholipids by oxidative stress--exceptional significance of cardiolipin. Free Radic Res 2010;44:135-145.
62 Heilbronn LK, Gan SK, Turner N, Campbell LV, Chisholm DJ: Markers of mitochondrial biogenesis and metabolism are lower in overweight and obese insulin-resistant subjects. J Clin Endocrinol Metab 2007;92:1467-1473.
63 Petersen KF, Dufour S, Befroy D, Garcia R, Shulman GI: Impaired mitochondrial activity in the insulin-resistant offspring of patients with type 2 diabetes. N Engl J Med 2004;350:664-671.
64 Lipina C, Macrae K, Suhm T, Weigert C, Blachnio-Zabielska A, Baranowski M, et al.: Mitochondrial Substrate Availability and its Role in Lipid-Induced Insulin Resistance and Proinflammatory Signalling in Skeletal Muscle. Diabetes 2013;62:3426-3436.
65 Harper JA, Dickinson K, Brand MD: Mitochondrial uncoupling as a target for drug development for the treatment of obesity. Obes Rev 2001;2:255-265.
66 Skulachev VP: Fatty acid circuit as a physiological mechanism of uncoupling of oxidative phosphorylation. FEBS Lett 1991;294:158-162.
67 Sparks LM, Gemmink A, Phielix E, Bosma M, Schaart G, Moonen-Kornips E, et al.: ANT1-mediated fatty acid-induced uncoupling as a target for improving myocellular insulin sensitivity. Diabetologia 2016;59:1030-1039.
68 Schrauwen P, Hesselink MK: The role of uncoupling protein 3 in fatty acid metabolism: protection against lipotoxicity? Proc Nutr Soc 2004;63:287-292.
69 Himms-Hagen J, Harper ME: Physiological role of UCP3 may be export of fatty acids from mitochondria when fatty acid oxidation predominates: an hypothesis. Exp Biol Med (Maywood) 2001;226:78-84.
70 Capel F, Cheraiti N, Acquaviva C, Henique C, Bertrand-Michel J, Vianey-Saban C, et al.: Oleate dose-dependently regulates palmitate metabolism and insulin signaling in C2C12 myotubes. Biochim Biophys Acta 2016;1861:2000-2010.
71 Palomer X, Pizarro-Delgado J, Barroso E, Vazquez-Carrera M: Palmitic and Oleic Acid: The Yin and Yang of Fatty Acids in Type 2 Diabetes Mellitus. Trends Endocrinol Metab 2018;29:178-190.
72 Kris-Etherton PM, Petersen KF, Van Horn L: Convincing evidence supports reducing saturated fat to decrease cardiovascular disease risk. BMJ Nutrition, Prevention & Health 2018;1:23-26.
73 de Lau LM, Bornebroek M, Witteman JC, Hofman A, Koudstaal PJ, Breteler MM: Dietary fatty acids and the risk of Parkinson disease: the Rotterdam study. Neurology 2005;64:2040-2045.